Author Manuscript

Author Manuscript

Author Manuscript

Author Manuscript

HHS Public Access

Author manuscript

Neurochem Int. Author manuscript; available in PMC 2018 October 01.

Published in final edited form as:

Neurochem Int. 2017 October ; 109: 24–33. doi:10.1016/j.neuint.2017.01.001.

Oxidative metabolism and Ca^{2+} handling in striatal mitochondria from YAC128 mice, a model of Huntington's disease

James Hamilton[1], **Tatiana Brustovetsky**[1], and **Nickolay Brustovetsky**[1,2]

[1]Department of Pharmacology and Toxicology, Indiana University School of Medicine

[2]Stark Neuroscience Research Institute, Indiana University School of Medicine

Abstract

The mechanisms implicated in the pathology of Huntington's disease (HD) remain not completely understood, although dysfunction of mitochondrial oxidative metabolism and Ca^{2+} handling have been suggested as contributing factors. However, in our previous studies with mitochondria isolated from the whole brains of HD mice, we found no evidence for defects in mitochondrial respiration and Ca^{2+} handling. In the present study, we used the YAC128 mouse model of HD to evaluate the effect of mHtt on respiratory activity and Ca^{2+} uptake capacity of mitochondria isolated from the striatum, the most vulnerable brain region in HD. Isolated, Percoll-gradient purified striatal mitochondria from YAC128 mice were free of cytosolic and ER contaminations, but retained attached mHtt. Both nonsynaptic and synaptic striatal mitochondria isolated from early symptomatic 2-month-old YAC128 mice had similar respiratory rates and Ca^{2+} uptake capacities compared with mitochondria from wild-type FVB/NJ mice. Consistent with the lack of difference in mitochondrial respiration, we found that the expression of several nuclear-encoded proteins in striatal mitochondria was similar between wild-type and YAC128 mice. Taken together, our data demonstrate that mHtt does not alter respiration and Ca^{2+} uptake capacity in striatal mitochondria isolated from YAC128 mice, suggesting that respiratory defect and Ca^{2+} uptake deficiency most likely do not contribute to striatal pathology associated with HD.

Keywords

Huntington's disease; mitochondria; striatum; respiration; calcium; YAC128

1. Introduction

Huntington's disease (HD) is a fatal neurodegenerative disorder characterized by a progressive decline of motor and cognitive functions (Roze et al., 2010). An increase in the

Correspondence: Nickolay Brustovetsky, PhD, Department of Pharmacology and Toxicology, Indiana University School of Medicine, 635 Barnhill Drive, Medical Science Building, Room 547, Indianapolis, IN 46202, Phone 317-278-9229, Fax 317-274-7714, nbrous@iu.edu.

The authors have no conflicts of interest.

Publisher's Disclaimer: This is a PDF file of an unedited manuscript that has been accepted for publication. As a service to our customers we are providing this early version of the manuscript. The manuscript will undergo copyediting, typesetting, and review of the resulting proof before it is published in its final citable form. Please note that during the production process errors may be discovered which could affect the content, and all legal disclaimers that apply to the journal pertain.

Author Manuscript Author Manuscript Author Manuscript Author Manuscript

number of CAG repeats to more than 35 in exon 1 of the *htt* gene has been proposed to be the genetic alteration leading to HD (MacDonald et al., 1993). This mutation leads to the expression of the mutated huntingtin protein (mHtt) which harbors an elongated polyglutamine (polyQ) domain near the N-terminus (MacDonald et al., 1993). Although the mutation linked to HD was identified more than 20 years ago, the precise mechanism of deleterious action of mHtt is still unclear. Among other mechanisms, bioenergetic abnormalities and altered mitochondrial Ca^{2+} handling have been suggested as potential contributors to neuronal dysfunction in HD (Giacomello et al., 2011; Polyzos and McMurray, 2016).

Earlier findings suggested abnormalities in mitochondrial respiration and defects in Ca^{2+} handling in mitochondria from HD mouse and cell models (Tabrizi et al., 2000; Damiano et al., 2013; Aidt et al., 2013; Panov et al., 2002; Choo et al., 2004; Lim et al., 2008). In our previous studies, we tested the possible deleterious effects of mHtt on mitochondrial oxidative metabolism and Ca^{2+} handling using isolated nonsynaptic and synaptic mitochondria from the whole brain of HD mice (Pellman et al., 2015; Hamilton et al., 2015; Hamilton et al., 2016). We tested mitochondrial functions using transgenic YAC128 mice, which express full-length human mHtt, and R6/2 mice, which express the N-terminal fragment of human mHtt (Slow et al., 2003). Despite our efforts, we did not find evidence for mitochondrial dysfunction using nonsynaptic and synaptic mitochondria isolated from both YAC128 and R6/2 mouse models of HD. In HD, different brain regions have different susceptibility to degeneration with striatum being most vulnerable, and the hippocampus and cerebellum remaining practically unaffected (Vonsattel and DiFiglia, 1998). Consequently, the use of mitochondria isolated from whole mouse brains could be a reason for our failure to detect mitochondrial dysfunction in HD mice.

Marked atrophy of the caudate nucleus and putamen represent the first features of brain pathology in HD (Vonsattel et al., 1985). Within the striatum, the GABAergic medium spiny neurons, which comprise about 95% of all neurons in the striatum, are the cell type that is most susceptible to degeneration (Han et al., 2010). Striatal loss is discernable in HD patients even before classical choreiform signs of HD appear (Bates et al., 2015). In this study, investigators used magnetic resonance imaging applied to clinically diagnosed prodromal HD patients and found that striatal atrophy precedes the onset of motor symptoms. Similar to the pathology found in HD patients, YAC128 mice display decreased number of striatal neurons and diminished striatal volume compared to wild-type mice (Slow et al., 2003; Pouladi et al., 2012). It is conceivable that mitochondrial defects contribute to neuronal dysfunction and eventual cell death of striatal neurons. In the present study, we assessed the respiratory activity and Ca^{2+} handling in mitochondria isolated exclusively from the striatal tissues of YAC128 mice. Consistent with our previously reported data, we found no evidence of mHtt-induced impairment of respiration and Ca^{2+} handling in striatal nonsynaptic and synaptic mitochondria isolated from brains of YAC128 mice.

Author Manuscript Author Manuscript Author Manuscript Author Manuscript

2. Materials and Methods

2.1 Materials

Pyruvate, malate, succinate, glutamate, ADP, and 2,4-dinitrophenol were purchased from Sigma (St. Louis, MO). Bovine serum albumin (BSA), free from free fatty acids, was from MP Biomedicals (Irvine, CA).

2.2 Animals and genotyping

All procedures with animals were performed in accordance with the Institutional Animal Care and Use Committee approved protocol. All efforts were made to minimize animal suffering, to reduce the number of animals used, and to utilize alternatives to in vivo techniques, if available. All animal experiments were carried out in accordance with the National Institutes of Health guide for the care and use of Laboratory animals (NIH Publications No. 80-23, revised 1978). Transgenic YAC128 mice as well as wild-type FVB/NJ mice were purchased from Jackson Laboratories (Bar Harbor, ME) and breeding colonies were established in the Laboratory Animal Resource Center at Indiana University School of Medicine, Indianapolis, IN. YAC128 mice express full-length human mHtt, including upstream and downstream regulatory elements, containing a polyglutamine (polyQ) region of 128 glutamines. Female FVB/NJ mice were bred with male YAC128 mice. Mice were housed under standard conditions with free access to food and water. In all of our experiments, we used early symptomatic 2-month-old YAC128 mice and FVB/NJ littermates. Every animal used for experiments was genotyped by PCR assay on tail DNA. PCR of tail DNA was carried out according to the protocol furnished by Jackson Laboratories with oligonucleotide primers oIMR6533 (GGCTGAGGAAGCTGAGGAG) and TmoIMR1594 (CCGCTCAGGTTCTGCTTTTA) (Invitrogen, Carlsbad, CA). The PCR reaction mixture was prepared with 1μL DNA template and 24μL Platinum PCR SuperMix (Invitrogen) containing 0.39μM of each primer for a total reaction volume of 25μL. Cycling conditions were 5 min at 95°C, 35 cycles of 30 s at 95°C, 30 s at 56°C, 60 s at 72°C, 10 min at 72°C. PCR reaction products were visualized on a 1.2% agarose gel run at 100 V for 60 min with Tris–acetate–EDTA running buffer containing 1X GelRedTM Nucleic Acid Gel Stain (Biotium, Hayward, CA).

2.3 Isolation of nonsynaptic and synaptic striatal mitochondria

Percoll gradient-purified striatal nonsynaptic and synaptic mitochondria from 2-month-old YAC128 and wild-type FVB/NJ littermates were isolated as previously described (Brustovetsky et al., 2002; Shalbuyeva et al., 2007). HD affects men and women equally (Novak and Tabrizi, 2010); therefore, throughout this study mice of both sexes were used. Brains from both males and females were pooled for the mitochondrial isolation. To prepare nonsynaptic mitochondria, the striata of nine FVB/NJ and YAC128 mice each were used for a single isolation procedure and for synaptic mitochondria 15 mice of each strain were used for a single isolation procedure (Brustovetsky et al., 2003). It was previously proposed that BSA may preclude mHtt from binding to the mitochondrial outer membrane (Panov et al., 2003), therefore, where indicated, BSA was omitted from solutions used in isolation procedures and from incubation medium. However, in our previous study, we showed that BSA does not displace mHtt from mitochondria (Pellman et al., 2015). Consequently, where

Author Manuscript Author Manuscript Author Manuscript Author Manuscript

indicated 0.1% BSA (free from fatty acids) was used in isolation solutions and incubation medium.

2.4 Immunoblotting

Brain homogenates, cytosolic fractions, and striatal isolated mitochondria that were previously treated with Proteinase Inhibitor Cocktail (Roche, Indianapolis, IN) were solubilized by incubation in NuPAGE LDS sample buffer (Invitrogen) plus a reducing agent at 70°C for 10 min. Either Bis-Tris Mops gels (4–12%, Invitrogen) or Tris-Acetate gels (3–8%, Invitrogen) were used to separate proteins by electrophoresis. Either 10 or 40μg protein per lane was loaded. Following electrophoresis, proteins were transferred to Hybond-ECL nitrocellulose membrane (Amersham Biosciences, Piscataway, NJ). Blots were incubated for 1 hour at room temperature in blocking solution of either 5% milk or 5% BSA dissolved in phosphate-buffered saline, pH 7.2, and 0.15% Triton X-100. Then, blots were incubated with one of the following primary antibodies: mouse monoclonal anti-polyQ 1C2 (mAB 1574, 1:3000, Millipore, Temecula, CA), rabbit polyclonal anti-calnexin (1:1200, Abcam, Cambridge, MA), rabbit monoclonal anti-MEK1/2 (1:2000, Pierce, Rockford, IL), mouse monoclonal anti-Complex I 39 kDa subunit (1:1000, Invitrogen), mouse monoclonal anti-Complex II 30 kDa subunit (1:1000, Invitrogen), mouse monoclonal anti-Complex II 70 kDa subunit (1:1000, Invitrogen), mouse monoclonal anti-aconitase 2 (1:1000, Abcam), rabbit polyclonal anti-manganese superoxide dismutase (MnSOD, 1:2000, Millipore), mouse monoclonal anti-ATP synthase α subunit (1:1000, Abcam), mouse monoclonal anti-CyD antibody (1:500, Calbiochem, San Diego, CA), mouse monoclonal anti-Complex IV (1:2500, Invitrogen), rabbit polyclonal anti-VDAC1 (1:1000, Calbiochem). Blots were incubated with either goat anti-mouse or goat anti-rabbit IgG (1:25000 or 1:20000, respectively) coupled with horseradish peroxidase (Jackson ImmunoResearch Laboratories, West Grove, PA) and developed with Supersignal West Pico chemiluminescent reagents (Pierce). Molecular mass markers See Blue Plus 2 Standards (Invitrogen) and HiMark Pre-stained High Molecular Weight Protein Standards (Invitrogen) were used for molecular mass determination. NIH ImageJ 1.48v software (http://rsb.info.nih.gov//ij) was used for densitometry.

2.5 Mitochondrial respiration

Mitochondrial respiration was measured with a Clark-type oxygen electrode during continuous stirring in a tightly sealed 0.4 ml chamber heated to 37°C. Experiments were performed in the standard incubation medium containing 125 mM KCl, 0.5 mM $MgCl_2$, 3 mM KH_2PO_4, 10 mM Hepes, pH 7.4, 10μM EGTA supplemented with either 3mM pyruvate plus 1 mM malate or 3 mM succinate plus 3 mM glutamate. Glutamate was used in experiments with succinate to prevent oxaloacetate-mediated inhibition of succinate dehydrogenase (Wojtczak, 1969; Brustovetsky and Dubinsky, 2000). Respiratory rates were calculated from the slopes of the oxygen consumption traces.

2.6 Mitochondrial Ca^{2+} uptake capacity

Mitochondrial Ca^{2+} uptake was measured under continuous stirring in a 0.3 ml chamber equipped with a miniature Ca^{2+}-selective electrode and heated to 37°C. Uptake of Ca^{2+} by mitochondria is indicated by a decrease in external Ca^{2+} in the chamber. The experiments

Author Manuscript Author Manuscript Author Manuscript Author Manuscript

were performed in the standard incubation medium supplemented with either 3 mM pyruvate plus 1 mM malate or 3 mM succinate plus 3 mM glutamate. As described previously, the incubation medium was also supplemented with 0.1 mM ADP and 1μM oligomycin in these experiments (Chalmers and Nicholls, 2003). Ca^{2+} was applied to isolated mitochondria in the form of 10μM $CaCl_2$ pulses.

2.7 Statistics

Statistical analysis of the experimental results consisted of unpaired *t*-test or one-way ANOVA followed by Bonferroni's *post hoc* test (GraphPad Prism® 4.0, GraphPad Software Inc., SanDiego, CA, USA). Data are shown as mean ± SEM of several independent experiments.

3. Results

3.1. Clasping phenotype of early symptomatic YAC128 mice

In this study, we used YAC128 mice which express full-length human mHtt with an expanded glutamine tract of 128 repeats under control of the endogenous human promoter (Slow, 2003). The mice ranged in age from 8–10 weeks and already showed signs of motor dysfunction manifested as clasping of the fore- and hind-limbs when suspended by the tail (Fig. 1A, B). This clasping behavior is characteristic of HD mice and has been previously reported (Mangiarini et al., 1996; Reddy et al., 1999). Since the mice exhibited this phenotype, it suggests that if altered mitochondrial respiration or Ca^{2+} handling contributed to such behavioral aberrations, we should be able to detect such defects in brain mitochondria isolated from these mice. For all experiments, age-matched genetic background FVB/NJ mice were used as control. Before all experiments, every mouse was genotyped by PCR on tail DNA to confirm the presence or absence of the transgene (Fig. 1C).

3.2. Expression of mHtt in striatal mitochondria and purity of mitochondrial preparations

Nonsynaptic mitochondria were derived from neuronal somata and glial cells whereas synaptic mitochondria were isolated from neuronal synaptic terminals and, therefore, were of exclusively neuronal origin. Figure 2A, B shows the absence of MEK1/2, a cytosolic marker, and calnexin, an endoplasmic reticulum (ER) marker, in mitochondrial fractions, suggesting the absence of cytosolic and ER contaminations. On the other hand, mitochondrial fractions contained augmented levels of Complex II, 70 kDa subunit (CII, 70) indicating mitochondrial enrichment in these fractions. Mitochondria from YAC128, but not FVB/NJ mice, contained mHtt detected with mouse monoclonal mHtt-specific antibody 1C2 (1:1000, mAb 1574, Millipore, Temecula, CA) that recognizes the polyglutamine stretch of the protein (Fig. 2C). This is consistent with our previous data (Hamilton et al., 2015) and with results from others (Choo et al., 2004). Huntingtin protein and its mutated form, mHtt, reside in the cytosol (Bates et al., 2015) and, therefore, the presence of mHtt in the mitochondrial fraction could be due to cytosolic contamination. However, because mitochondrial fractions did not contain detectable amounts of cytosolic contamination, mHtt present in mitochondrial fractions (Fig. 2C) was unlikely to be the result of cytosolic contamination (Fig. 2A, B). Thus, in our study we used striatal nonsynaptic and synaptic

Author Manuscript Author Manuscript Author Manuscript Author Manuscript

mitochondria which were essentially free from cytosolic and ER contaminations and contained mHtt attached to mitochondria.

3.3. Respiration of nonsynaptic and synaptic striatal mitochondria from YAC128 mice

In our initial experiments, we used striatal nonsynaptic mitochondria fueled with 3 mM pyruvate and 1 mM malate, a combination of Complex I-linked substrates. Mitochondrial respiratory rates were measured under various conditions: basal mitochondrial respiration in the presence of only substrates (V_2), ADP-stimulated respiration (V_3, 300μM ADP), respiration following ADP depletion (V_4), and maximal, 2,4-dinitrophenol (2,4-DNP)-stimulated respiration (V_{DNP}, 60μM 2,4-DNP). Earlier, it was reported that the functional difference between mitochondria from HD and wild-type animals could be reliably detected only in the absence of BSA (Panov et al., 2003). In the aforementioned study, BSA eliminated the difference and it was proposed that BSA displaces mHtt from the mitochondrial outer membrane. Consequently, BSA was omitted from all isolation and incubation solutions in our experiments shown in Figure 3. In these experiments, striatal mitochondria isolated from YAC128 and FVB/NJ mice had similar respiratory rates under every experimental condition.

Previously, it was shown that inhibition of Complex II with 3-nitropropionic acid recapitulated HD pathology in animals (Brouillet et al., 1999) and it was demonstrated that activity of Complex II is decreased in striatum of HD patients and in HD mouse striatal neurons (Benchoua et al., 2006). Correspondingly, in our subsequent experiments, we used 3 mM succinate as a mitochondrial substrate in combination with 3 mM glutamate to remove oxaloacetate via transamination reaction and thus prevent oxaloacetate-mediated inhibition of Complex II (Wojtczak, 1969; Brustovetsky and Dubinsky, 2000). In addition, the incubation medium was supplemented with 0.1% BSA (free from fatty acids) to preserve mitochondrial integrity and improve mitochondrial functionality (Lai and Clark, 1989). In our previous study, we found that incubation of isolated mitochondria with 0.1% BSA failed to displace mHtt from the organelles (Pellman et al., 2015) and, therefore, we expected to detect mHtt effects on mitochondria despite the presence of BSA. In these experiments, we used nonsynaptic and synaptic mitochondria isolated from striata of YAC128 and FVB/NJ mice. Similar to our previously described experiments (Fig. 3), we did not find any difference in respiratory activity between mitochondria from YAC128 and wild-type FVB/NJ mice (Fig. 4).

3.4. Expression of nuclear-encoded proteins in mitochondria from YAC128 and wild-type mice

Recently, inhibition of protein import machinery in mitochondria from HD mice was reported and suggested to be a possible cause of bioenergetic deficit in HD (Yano et al., 2014). The decrease in the levels of nuclear-encoded mitochondrial proteins seems to be a logical consequence of inhibition of mitochondrial import into mitochondria. However, this was not tested in the recent study (Yano et al., 2014). In our previous work with mitochondria isolated from the whole brain of YAC128 and wild-type FVB/NJ mice we did not find any difference in expression of nuclear-encoded proteins in mitochondria isolated from the whole brains (Hamilton et al., 2015). In the present study, we evaluated the levels

Author Manuscript Author Manuscript Author Manuscript Author Manuscript

of protein expression in striatal nonsynaptic and synaptic mitochondria from YAC128 and FVB/NJ mice using immunoblotting followed by densitometry (Fig. 5). In these experiments, we did not find a difference in expression of randomly chosen nuclear-encoded proteins located in the inner membrane or matrix of mitochondria from YAC128 and FVB/NJ mice. We also did not find a difference in expression of VDAC1, a protein of the mitochondrial outer membrane.

3.5. Ca^{2+} uptake capacity of striatal nonsynaptic and synaptic mitochondria from YAC128 and wild-type mice

Mitochondrial Ca^{2+} uptake plays an essential role in removal of excessive Ca^{2+} from the cytosol (Bernardi, 1999) and therefore is essential for maintenance of Ca^{2+} homeostasis in the cell and for cell survival (Bernardi and Rasola, 2007). Ca^{2+} accumulation in mitochondria is restricted by induction of the mitochondrial permeability transition pore that depolarizes mitochondria and thereby limits their ability to accumulate additional Ca^{2+} (Bernardi, 1999). Earlier, it was reported that mitochondria from HD mouse and cell models have decreased Ca^{2+} uptake capacity compared with mitochondria from wild-type animals and cells (Panov et al., 2002; Milakovic et al., 2006; Lim et al., 2008; Gellerich et al., 2008). However, recently we assessed Ca^{2+} uptake capacity in mitochondria isolated from the whole brains of YAC128 and R6/2 mice and did not find a difference compared to mitochondria from corresponding age-matched wild-type animals (Pellman et al., 2015; Hamilton et al., 2016). In the present study, we evaluated Ca^{2+} uptake capacity in striatal mitochondria from YAC128 and their genetic background FVB/NJ mice. We used nonsynaptic mitochondria incubated without BSA and fueled with a combination of 3 mM pyruvate and 1 mM malate or with a combination of 3 mM succinate and 3 mM glutamate (Fig. 6A, B). In both cases, Ca^{2+} uptake capacities of mitochondria from YAC128 and FVB/NJ mice were similar. In the latter case, supplementing incubation medium with BSA significantly increased Ca^{2+} uptake capacity of mitochondria from both YAC128 and FVB/NJ mice without revealing any difference between mitochondria from these animals (Fig. 6C). Figure 6D shows statistical analysis of these experiments.

Next, we tested striatal synaptic mitochondria from YAC128 and FVB/NJ mice (Fig. 7). Mitochondria were fueled with a combination of 3 mM succinate and 3 mM glutamate and incubated without BSA. We did not find a difference in Ca^{2+} uptake capacity in striatal synaptic mitochondria from YAC128 and FVB/NJ mice (Fig. 7A). Addition of BSA to the incubation medium significantly increased Ca^{2+} uptake capacity in mitochondria from both YAC128 and FVB/NJ mice (Fig. 7B). Interestingly, under these conditions striatal synaptic mitochondria from YAC128 mice accumulated even more Ca^{2+} than mitochondria from wild-type animals. Figure 7C shows statistical analysis of these experiments. Taken together, evaluation of mitochondrial Ca^{2+} uptake capacity did not provide evidence for defects in Ca^{2+} handling by striatal mitochondria from YAC128 mice.

4. Discussion

The role of mitochondrial dysfunction in HD pathogenesis has been investigated in many studies with contradictory results (Brustovetsky, 2016). This controversy may arise from

Author Manuscript Author Manuscript Author Manuscript Author Manuscript

variations in experimental models of HD and techniques used in these studies. Nevertheless, all of these studies may provide important information regarding possible mechanisms involved in HD pathogenesis. In our recent studies, we showed that nonsynaptic and synaptic mitochondria isolated from whole brains of YAC128 and R6/2 mice have similar respiratory rates and Ca^{2+} uptake capacities compared to mitochondria from corresponding genetic background animals: FVB/NJ and B6CBAF1/J mice, respectively (Pellman et al., 2015; Hamilton et al., 2015; Hamilton et al., 2016). The results produced in experiments with isolated mitochondria were substantiated in studies with striatal neurons in culture. In HD, striatum is the most vulnerable brain region whereas hippocampus and cerebellum remain practically intact (Vonsattel and DiFiglia, 1998). The use of mitochondria isolated from whole brains was a limitation of our previous studies because contribution from mitochondria from unaffected brain regions may have obscured deficiencies of striatal mitochondria. In the present study, we used nonsynaptic and synaptic mitochondria isolated exclusively from striata of 8–10 week-old YAC128 and FVB/NJ mice. The results produced in the present study are consistent with our data reported previously (Pellman et al., 2015; Hamilton et al., 2015; Hamilton et al., 2016). We did not find evidence for alterations in expression of nuclear-encoded mitochondrial proteins and for impairment of mitochondrial respiration and Ca^{2+} uptake capacity in striatal mitochondria from YAC128 mice compared to mitochondria from FVB/NJ mice. These findings argue against mitochondrial dysfunction as a contributing factor in HD pathogenesis.

Relatively simple and straightforward experiments with isolated mitochondria provide a unique opportunity to examine the effect of mHtt on mitochondrial functions under well-defined conditions. The fact that brain mitochondria isolated from HD mouse models retain attached mHtt and the possibility of creating well-defined experimental conditions represent the major strengths of this approach. However, such an approach has some weaknesses. Isolated mitochondria are removed from their natural environment and this may affect their functions. Therefore, it is important to verify data obtained with isolated mitochondria using more complex cell model of cultured primary neurons. In our previous studies, we examined oxidative metabolism and mitochondrial Ca^{2+} handling in cultured striatal neurons from YAC128 and FVB/NJ mice (Pellman et al., 2015; Hamilton et al., 2015). In the present study, we assessed respiration and Ca^{2+} uptake capacity in striatal nonsynaptic and synaptic mitochondria isolated from these mice. Although, two-month-old YAC128 mice already demonstrate clasping behavior, an early symptom associated with mHtt expression (Mangiarini et al., 1996; Reddy et al., 1999; Hamilton et al., 2015), our data obtained with cultured neurons and isolated mitochondria from YAC128 mice provide no evidence for mitochondrial impairment.

Mitochondrial respiration generates an electrochemical proton gradient across the mitochondrial inner membrane which is utilized to synthesize ATP in the process of oxidative phosphorylation and to transport Ca^{2+} into the mitochondrial matrix. Consequently, impairment of mitochondrial respiration may affect both oxidative phosphorylation and Ca^{2+} uptake. There are several reports suggesting mitochondrial respiratory deficits in various HD models (Tabrizi et al., 2000; Damiano et al., 2013; Aidt et al., 2013). However, our recent studies demonstrated the lack of defects in oxidative metabolism in mitochondria isolated from the whole HD brains and in cultured cortical and

Author Manuscript Author Manuscript Author Manuscript Author Manuscript

striatal neurons derived from HD mice (Hamilton et al., 2015; Hamilton et al., 2016). In our current study, we did not find a difference in ADP-stimulated respiration and in uncoupled respiration stimulated by 2,4-DNP. This suggests that the oxidative phosphorylation system and electron transport chain are not affected by mHtt. Similar respiratory activities were observed with both malate plus pyruvate, Complex I substrates, and with succinate, a Complex II substrate. This suggests that Complex I and Complex II of electron transport chain are not impaired by mHtt. Our findings presented here are consistent with previously reported data. In early studies, Guidetti et al. did not detect alterations in activity of electron transport chain in the striatum and cerebral cortex of HD48 and HD89 mice, expressing full-length mHtt with 48 or 89 glutamines, respectively, compared to wild-type mice (Guidetti et al., 2001). In experiments with cultured striatal neurons from 15–17 week-old heterozygous *Hdh*150 mice, cell respiratory activities were found to be similar (Oliveira et al., 2007). Olah et al. found that the activities of Complexes I–IV in brain mitochondria from 20-week-old transgenic N171-82Q mice were not diminished compared to mitochondria from wild-type animals (Olah et al., 2008). Gouarne et al. did not find a difference in respiration of cultured striatal neurons from heterozygous transgenic BACHD rats compared to wild-type neurons, when cells were incubated in the presence of 25 mM glucose and 1 mM pyruvate (Gouarne et al., 2013). In experiments with *STHdh*$^{Q111/Q111}$ cells, mitochondrial pathways were not significantly altered and the obtained data uniformly refuted a view of direct deleterious mHtt effect on mitochondria (Lee et al., 2007). The direct measurements of oxidative metabolism in striatum of HD patients and age-matched controls using positron emission tomography failed to find a difference that argues against a defect in mitochondrial oxidative phosphorylation and mitochondrial electron transport chain activity (Powers et al., 2007). Finally, Ismailoglu et al. studied mouse embryonic stem cells expressing wild-type and 140Q-mHtt and found no difference in cellular bioenergetics of these cell lines (Ismailoglu et al., 2014). Collectively, these results suggest the lack of overt respiratory defects in HD mitochondria.

A recent paper by Yano et al. described a series of well-designed experiments demonstrating inhibition of mitochondrial protein import machinery by mHtt that might lead to respiratory defects (Yano et al., 2014). However, the authors did not examine the levels of expression of nuclear-encoded mitochondrial proteins to demonstrate consequences of suppressed protein import into mitochondria. Moreover, the authors failed to detect a decrease in respiratory activity in mitochondria isolated from R6/2 mice (Yano et al., 2014). Although we did not assess activity of protein import machinery in striatal mitochondria from YAC128 mice, our data unequivocally demonstrate the lack of respiratory deficits and show the absence of alterations in protein expression in mitochondria from YAC128 mice. Taken together, these data suggest that if protein import in mitochondria of HD mice is suppressed, this, nevertheless, does not affect the level of expression of mitochondrial nuclear encoded proteins and, consequently, does not affect mitochondrial respiration.

Mitochondria possess Ca^{2+} channels, historically known as “calcium uniporter”, that allows Ca^{2+} influx into the mitochondrial matrix driven by high membrane potential, negative inside of the organelle (Bernardi, 1999). Inside of mitochondria, elevated Ca^{2+} can interact with inorganic phosphate and precipitate in the form of hydroxyapatite (Chalmers and Nicholls, 2003). This allows for the large Ca^{2+} accumulation in mitochondria. The ability of

Author Manuscript Author Manuscript Author Manuscript Author Manuscript

mitochondria to accumulate significant amounts of Ca^{2+} is important for maintenance of Ca^{2+} homeostasis in the cell (Bernardi and Rasola, 2007). Ca^{2+} accumulation in mitochondria is limited by induction of the mitochondrial permeability transition pore that depolarizes mitochondria and prevents further Ca^{2+} uptake (Bernardi, 1999). In early studies, decreased Ca^{2+} uptake capacity in mitochondria isolated from HD mouse and cell models was reported, and it was proposed to contribute to HD pathogenesis by affecting Ca^{2+} homeostasis in neurons (Panov et al., 2002; Milakovic et al., 2006; Lim et al., 2008; Gellerich et al., 2008). However, other investigators failed to find a decrease in mitochondrial Ca^{2+} uptake capacity in mitochondria exposed to mHtt with an elongated polyQ stretch (Oliveira et al., 2007; De et al., 2016). In these studies, the authors either did not find a difference between mitochondria from HD and wild-type animals or they found a paradoxical increase in Ca^{2+} accumulation in mitochondria from HD mice. Our recent studies with nonsynaptic and synaptic mitochondria isolated from the whole brain of YAC128 and R6/2 mice and with cultured neurons from these animals substantiate these observations (Pellman et al., 2015; Hamilton et al., 2016). The results presented in this paper demonstrate the lack impairment of Ca^{2+} handling in nonsynaptic and synaptic mitochondria isolated from striata of YAC128 mice and support previous findings indicating the lack of Ca^{2+} accumulation defect in mitochondria from HD mice.

The experiments with isolated mitochondria and cultured neurons provide valuable information about possible effects of mHtt. However, *in vivo* measurements of brain respiratory activity may further enhance our understanding of potential defects in oxidative metabolism in HD. A recent paper by Lou et al. described elegant experiments with the use of ^{17}O magnetic resonance spectroscopy aimed at assessing cerebral mitochondrial respiratory activity in R6/2 mice *in vivo* (Lou et al., 2016). In this study, the authors did not find a difference in basal striatal oxygen consumption rate in symptomatic R6/2 mice at rest. Inhibition of oxidative phosphorylation with oligomycin resulted in a similar decrease in respiration, suggesting similar phosphorylation capacity and coupling of oxidative phosphorylation in HD and wild-type mice. Yet, after injection of the uncoupler 2,4-DNP, the authors found a negligible (about 15%), but statistically significant, decrease in respiratory responses in both striatum and cortex of R6/2 mice compared with respiratory responses of corresponding brain tissues in wild-type animals (Lou et al., 2016). The physiological significance of this difference is not evident but it is clear that such conditions (2,4-DNP-induced stimulation) do not take place in real life. The ambiguity of the small difference in uncoupled respiration is supported by the fact that natural, sensory stimulation-induced elevation in respiration measured with photoacoustical microscopy (Yao et al., 2015) is weaker than 2,4-DNP-induced increase in oxygen consumption. Thus, importance and relevance of small decreases in 2,4-DNP stimulated respiration of mitochondria from HD mice is not obvious.

Overall, our current data obtained with striatal nonsynaptic and synaptic mitochondria from YAC128 mice and previously published data with whole-brain mitochondria and cultured striatal and cortical neurons from YAC128 and R6/2 mice (Pellman et al., 2015; Hamilton et al., 2015; Hamilton et al., 2016) do not provide evidence for mitochondrial respiratory deficiency and defects in mitochondrial Ca^{2+} handling. Other, mechanisms such as

Author Manuscript Author Manuscript Author Manuscript Author Manuscript

alterations in mitochondrial dynamics, may play more important roles in HD pathogenesis and, consequently, may need greater attention.

Acknowledgments

This study was supported by NIH/NINDS grant R01 NS078008 and Biomedical Research Grant from Indiana University to N.B.

References

Aidt FH, Nielsen SM, Kanters J, Pesta D, Nielsen TT, Norremolle A, … Hagen CM. Dysfunctional mitochondrial respiration in the striatum of the Huntington's disease transgenic R6/2 mouse model. PLoS Curr. 2013:5.

Bates GP, Dorsey R, Gusella JF, Hayden MR, Kay C, Leavitt BR, … Tabrizi SJ. Huntington disease. Nat Rev Dis Primers. 2015; 1:15005. [PubMed: 27188817]

Benchoua A, Trioulier Y, Zala D, Gaillard MC, Lefort N, Dufour N, … Brouillet E. Involvement of mitochondrial complex II defects in neuronal death produced by N-terminus fragment of mutated huntingtin. Mol Biol Cell. 2006; 17(4):1652–1663. [PubMed: 16452635]

Bernardi P. Mitochondrial transport of cations: channels, exchangers, and permeability transition. Physiol Rev. 1999; 79(4):1127–1155. [PubMed: 10508231]

Bernardi P, Rasola A. Calcium and cell death: the mitochondrial connection. Subcell Biochem. 2007; 45:481–506. [PubMed: 18193649]

Brouillet E, Conde F, Beal MF, Hantraye P. Replicating Huntington's disease phenotype in experimental animals. Prog Neurobiol. 1999; 59(5):427–468. [PubMed: 10515664]

Brustovetsky N. Mutant Huntingtin and Elusive Defects in Oxidative Metabolism and Mitochondrial Calcium Handling. Mol Neurobiol. 2016; 53(5):2944–2953. [PubMed: 25941077]

Brustovetsky N, Brustovetsky T, Jemmerson R, Dubinsky JM. Calcium-induced cytochrome c release from CNS mitochondria is associated with the permeability transition and rupture of the outer membrane. J Neurochem. 2002; 80(2):207–218. [PubMed: 11902111]

Brustovetsky N, Brustovetsky T, Purl KJ, Capano M, Crompton M, Dubinsky JM. Increased susceptibility of striatal mitochondria to calcium-induced permeability transition. J Neurosci. 2003; 23(12):4858–4867. [PubMed: 12832508]

Brustovetsky N, Dubinsky JM. Dual responses of CNS mitochondria to elevated calcium. J Neurosci. 2000; 20(1):103–113. [PubMed: 10627586]

Chalmers S, Nicholls DG. The relationship between free and total calcium concentrations in the matrix of liver and brain mitochondria. J Biol Chem. 2003; 278(21):19062–19070. [PubMed: 12660243]

Choo YS, Johnson GV, MacDonald M, Detloff PJ, Lesort M. Mutant huntingtin directly increases susceptibility of mitochondria to the calcium-induced permeability transition and cytochrome c release. Hum Mol Genet. 2004; 13(14):1407–1420. [PubMed: 15163634]

Damiano M, Diguet E, Malgorn C, D'Aurelio M, Galvan L, Petit F, … Brouillet E. A role of mitochondrial complex II defects in genetic models of Huntington's disease expressing N-terminal fragments of mutant huntingtin. Hum Mol Genet. 2013; 22(19):3869–3882. [PubMed: 23720495]

De MA, Scarlatti C, Costiniti V, Primerano S, Lopreiato R, Cali T, … Carafoli E. Calcium handling by endoplasmic reticulum and mitochondria in a cell model of Huntington's disease. PLoS Curr. 2016:8.

Gellerich FN, Gizatullina ZZ, Nguyen HP, Trumbeckaite S, Vielhaber S, Seppet E, … Striggow F. Impaired regulation of brain mitochondria by extramitochondrial Ca2+ in transgenic Huntington disease rats. J Biol Chem. 2008; 283(45):30715–30724. [PubMed: 18606820]

Giacomello M, Hudec R, Lopreiato R. Huntington's disease, calcium, and mitochondria. Biofactors. 2011; 37(3):206–218. [PubMed: 21674644]

Gouarne C, Tardif G, Tracz J, Latyszenok V, Michaud M, Clemens LE, … Pruss RM. Early deficits in glycolysis are specific to striatal neurons from a rat model of huntington disease. PLoS ONE. 2013; 8(11):e81528. [PubMed: 24303051]

Author Manuscript Author Manuscript Author Manuscript Author Manuscript

Guidetti P, Charles V, Chen EY, Reddy PH, Kordower JH, Whetsell WO Jr, … Tagle DA. Early degenerative changes in transgenic mice expressing mutant huntingtin involve dendritic abnormalities but no impairment of mitochondrial energy production. Exp Neurol. 2001; 169(2): 340–350. [PubMed: 11358447]

Hamilton J, Pellman JJ, Brustovetsky T, Harris RA, Brustovetsky N. Oxidative metabolism in YAC128 mouse model of Huntington's disease. Hum Mol Genet. 2015; 24(17):4862–4878. [PubMed: 26041817]

Hamilton J, Pellman JJ, Brustovetsky T, Harris RA, Brustovetsky N. Oxidative metabolism and Ca2+ handling in isolated brain mitochondria and striatal neurons from R6/2 mice, a model of Huntington's disease. Hum Mol Genet. 2016; 25(13):2762–2775. [PubMed: 27131346]

Han I, You Y, Kordower JH, Brady ST, Morfini GA. Differential vulnerability of neurons in Huntington's disease: The role of cell type-specific features. J Neurochem. 2010; 113(5):1073–1091. [PubMed: 20236390]

Ismailoglu I, Chen Q, Popowski M, Yang L, Gross SS, Brivanlou AH. Huntingtin protein is essential for mitochondrial metabolism, bioenergetics and structure in murine embryonic stem cells. Dev Biol. 2014; 391(2):230–240. [PubMed: 24780625]

Lai, JCK., Clark, JB. Isolation and characterization of synaptic and nonsynaptic mitochondria from mammalian brain. In: Boulton, AA.Baker, GB., Butterworth, RF., editors. Neuromethods. Humana Press; Clifton, NJ: 1989. p. 43-98.

Lee JM, Ivanova EV, Seong IS, Cashorali T, Kohane I, Gusella JF, … MacDonald ME. Unbiased gene expression analysis implicates the huntingtin polyglutamine tract in extra-mitochondrial energy metabolism. PLoS Genet. 2007; 3(8):e135. [PubMed: 17708681]

Lim D, Fedrizzi L, Tartari M, Zuccato C, Cattaneo E, Brini M, … Carafoli E. Calcium homeostasis and mitochondrial dysfunction in striatal neurons of Huntington disease. J Biol Chem. 2008; 283(9):5780–5789. [PubMed: 18156184]

Lou S, Lepak VC, Eberly LE, Roth B, Cui W, Zhu XH, … Dubinsky JM. Oxygen consumption deficit in Huntington disease mouse brain under metabolic stress. Hum Mol Genet. 2016; 25(13):2813–2826. [PubMed: 27193167]

MacDonald ME, Ambrose CM, Duyao MP, Myers RH, Lin C, Srinidhi L, … Harper PS. A novel gene containing a trinucleotide repeat that is expanded and unstable on Huntington's disease chromosomes. Cell. 1993; 72(6):971–983. [PubMed: 8458085]

Mangiarini L, Sathasivam K, Seller M, Cozens B, Harper A, Hetherington C, … Bates GP. Exon 1 of the HD gene with an expanded CAG repeat is sufficient to cause a progressive neurological phenotype in transgenic mice. Cell. 1996; 87(3):493–506. [PubMed: 8898202]

Milakovic T, Quintanilla RA, Johnson GV. Mutant huntingtin expression induces mitochondrial calcium handling defects in clonal striatal cells: functional consequences. J Biol Chem. 2006; 281(46):34785–34795. [PubMed: 16973623]

Novak MJ, Tabrizi SJ. Huntington's disease. BMJ. 2010; 340:34–40.

Olah J, Klivenyi P, Gardian G, Vecsei L, Orosz F, Kovacs GG, … Ovadi J. Increased glucose metabolism and ATP level in brain tissue of Huntington's disease transgenic mice. FEBS J. 2008; 275(19):4740–4755. [PubMed: 18721135]

Oliveira JM, Jekabsons MB, Chen S, Lin A, Rego AC, Goncalves J, … Nicholls DG. Mitochondrial dysfunction in Huntington's disease: the bioenergetics of isolated and in situ mitochondria from transgenic mice. J Neurochem. 2007; 101(1):241–249. [PubMed: 17394466]

Panov AV, Burke JR, Strittmatter WJ, Greenamyre JT. In vitro effects of polyglutamine tracts on Ca2+-dependent depolarization of rat and human mitochondria: relevance to Huntington's disease. Arch Biochem Biophys. 2003; 410(1):1–6. [PubMed: 12559971]

Panov AV, Gutekunst CA, Leavitt BR, Hayden MR, Burke JR, Strittmatter WJ, … Greenamyre JT. Early mitochondrial calcium defects in Huntington's disease are a direct effect of polyglutamines. Nat Neurosci. 2002; 5(8):731–736. [PubMed: 12089530]

Pellman JJ, Hamilton J, Brustovetsky T, Brustovetsky N. Ca(2+) handling in isolated brain mitochondria and cultured neurons derived from the YAC128 mouse model of Huntington's disease. J Neurochem. 2015; 134(4):652–667. [PubMed: 25963273]

Author Manuscript Author Manuscript Author Manuscript Author Manuscript

Polyzos AA, McMurray CT. The chicken or the egg: Mitochondrial dysfunction and oxidative damage as a cause or consequence of toxicity in Huntington's disease. Mech Ageing Dev. 2016; doi: 10.1016/j.mad.2016.09.003

Pouladi MA, Stanek LM, Xie Y, Franciosi S, Southwell AL, Deng Y. Marked differences in neurochemistry and aggregates despite similar behavioural and neuropathological features of Huntington disease in the full-length BACHD and YAC128 mice. Hum Mol Genet. 2012; 21(10): 2219–2232. … the last author. [PubMed: 22328089]

Powers WJ, Videen TO, Markham J, McGee-Minnich L, Antenor-Dorsey JV, Hershey T, Perlmutter JS. Selective defect of in vivo glycolysis in early Huntington's disease striatum. Proc Natl Acad Sci USA. 2007; 104(8):2945–2949. [PubMed: 17299049]

Reddy PH, Charles V, Williams M, Miller G, Whetsell WO Jr, Tagle DA. Transgenic mice expressing mutated full-length HD cDNA: a paradigm for locomotor changes and selective neuronal loss in Huntington's disease. Philos Trans R Soc Lond B Biol Sci. 1999; 354(1386):1035–1045. [PubMed: 10434303]

Roze E, Bonnet C, Betuing S, Caboche J. Huntington's disease. Adv Exp Med Biol. 2010; 685:45–63. [PubMed: 20687494]

Shalbuyeva N, Brustovetsky T, Brustovetsky N. Lithium desensitizes brain mitochondria to calcium, antagonizes permeability transition, and diminishes cytochrome C release. J Biol Chem. 2007; 282(25):18057–18068. [PubMed: 17485418]

Slow EJ, van Raamsdonk J, Rogers D, Coleman SH, Graham RK, Deng Y, … Hayden MR. Selective striatal neuronal loss in a YAC128 mouse model of Huntington disease. Hum Mol Genet. 2003; 12(13):1555–1567. [PubMed: 12812983]

Tabrizi SJ, Workman J, Hart PE, Mangiarini L, Mahal A, Bates G, … Schapira AH. Mitochondrial dysfunction and free radical damage in the Huntington R6/2 transgenic mouse. Ann Neurol. 2000; 47(1):80–86. [PubMed: 10632104]

Vonsattel JP, DiFiglia M. Huntington disease. J Neuropathol Exp Neurol. 1998; 57(5):369–384. [PubMed: 9596408]

Vonsattel JP, Myers RH, Stevens TJ, Ferrante RJ, Bird ED, Richardson EP Jr. Neuropathological classification of Huntington's disease. J Neuropathol Exp Neurol. 1985; 44(6):559–577. [PubMed: 2932539]

Wojtczak AB. Inhibitory action of oxaloacetate on succinate oxidation in rat-liver mitochondria and the mechanism of its reversal. Biochim Biophys Acta. 1969; 172(1):52–65. [PubMed: 4387597]

Yano H, Baranov SV, Baranova OV, Kim J, Pan Y, Yablonska S, … Friedlander RM. Inhibition of mitochondrial protein import by mutant huntingtin. Nat Neurosci. 2014; 17(6):822–831. [PubMed: 24836077]

Yao J, Wang L, Yang JM, Maslov KI, Wong TT, Li L, … Wang LV. High-speed label-free functional photoacoustic microscopy of mouse brain in action. Nat Methods. 2015; 12(5):407–410. [PubMed: 25822799]

Author Manuscript Author Manuscript Author Manuscript Author Manuscript

Highlights

- Respiration and Ca^{2+} capacity of striatal mitochondria from YAC128 mice were tested
- Mutant huntingtin failed to affect striatal mitochondrial respiration
- Mutant huntingtin did not alter expression of nuclear-encoded mitochondrial proteins
- Mutant huntingtin failed to diminish mitochondrial Ca^{2+} uptake capacity

Author Manuscript Author Manuscript Author Manuscript Author Manuscript

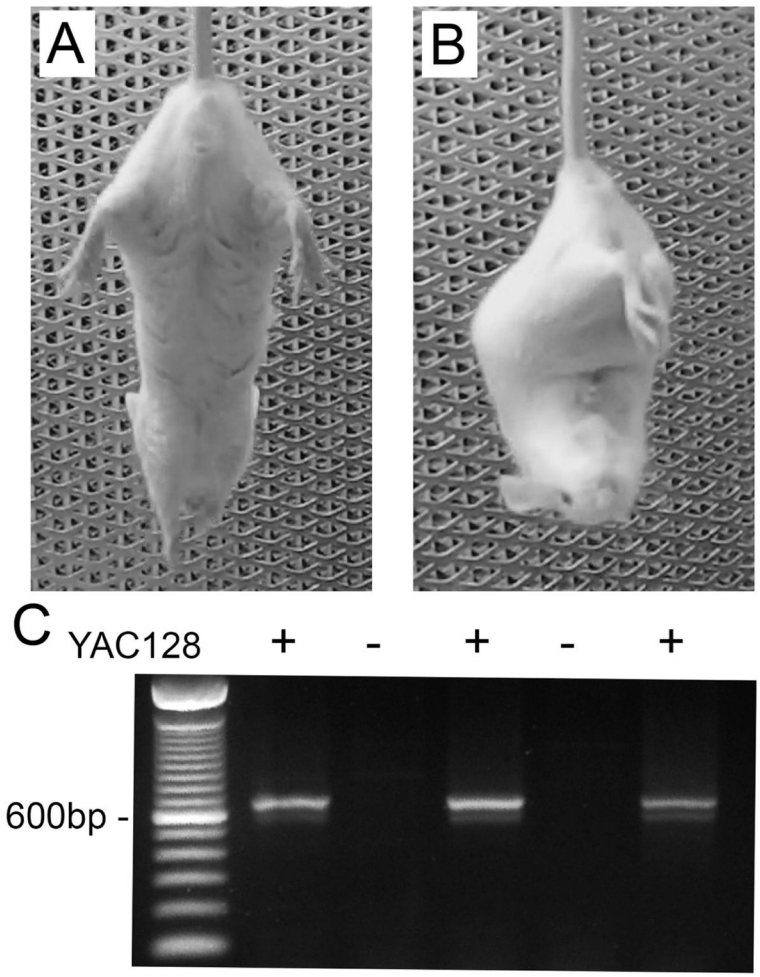

Figure 1.

Clasping phenotype of 8-week-old YAC128 mouse and representative genotyping. (**A**) Typical response of a wild-type (WT) FVB/NJ mouse during suspension by the tail whereby the mouse maintains extension of the fore- and hind-limbs away from the body. (**B**) Usual clasping posture of an 8-week-old YAC128 mouse with retraction of the limbs toward the center of the body. (**C**) Representative genotyping data following PCR of DNA from tail tissue of WT and YAC128 mice.

Author Manuscript Author Manuscript Author Manuscript Author Manuscript

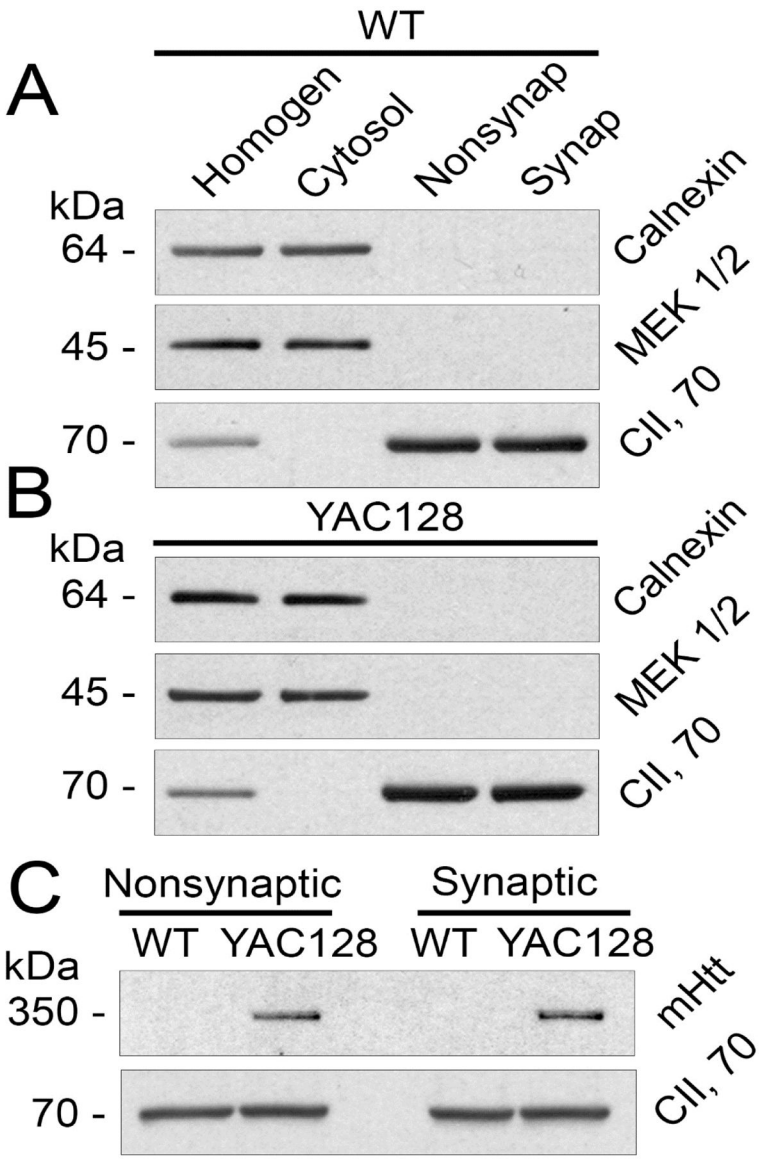

Figure 2.

Purity of striatal nonsynaptic (Nonsynap) and synaptic (Synap) mitochondria isolated from FVB/NJ (**A**) and YAC128 (**B**) mice and detection of mHtt in mitochondrial fractions (**C**). In **A** and **B**, purity of striatal mitochondrial fraction was assessed by western blotting. Homogenates (Homogen), cytosolic, and mitochondrial fractions were analyzed using antibodies against calnexin (ER marker), MEK1/2 (cytosolic marker), and the 70 kDa subunit of Complex II (mitochondrial marker). In **C**, mHtt was detected as a single band exclusively in samples from YAC128 mice using the mouse monoclonal anti-polyQ antibody 1C2. The 70 kDa subunit of Complex II was used as a mitochondrial marker and a loading control.

Author Manuscript Author Manuscript Author Manuscript Author Manuscript

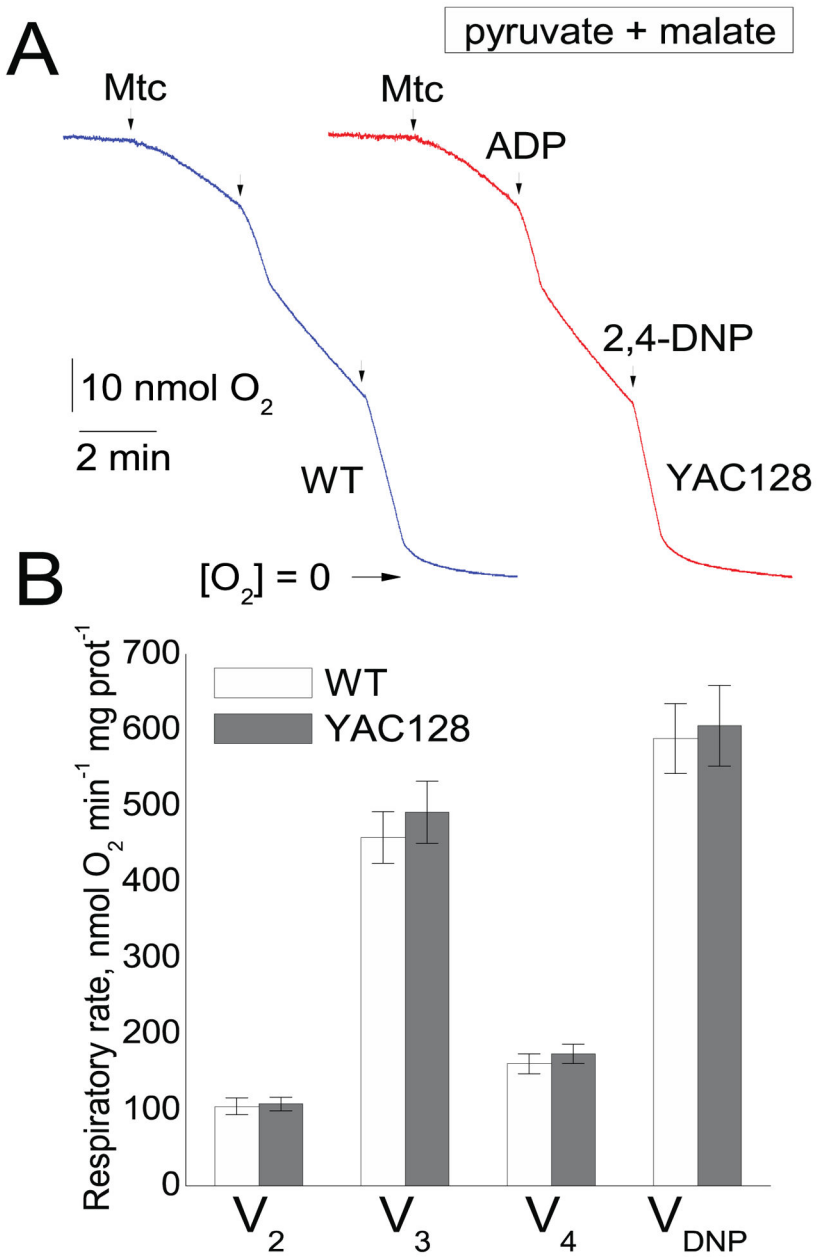

Figure 3.

Respiratory activity of striatal nonsynaptic mitochondria isolated from 2-month-old FVB/NJ (blue trace) and YAC128 (red trace) mice. In **A**, representative traces of oxygen consumption by striatal nonsynaptic mitochondria. Where indicated, mitochondria (30μg protein), 300μM ADP, or 60μM 2,4-dinitrophenol (2,4-DNP) were added. The incubation medium was supplemented with the Complex I substrates pyruvate (3 mM) plus malate (1 mM). In **B**, the pooled group results demonstrating respiratory rates of striatal nonsynaptic mitochondria. Data are mean ± SEM, n = 5.

Author Manuscript
Author Manuscript
Author Manuscript
Author Manuscript

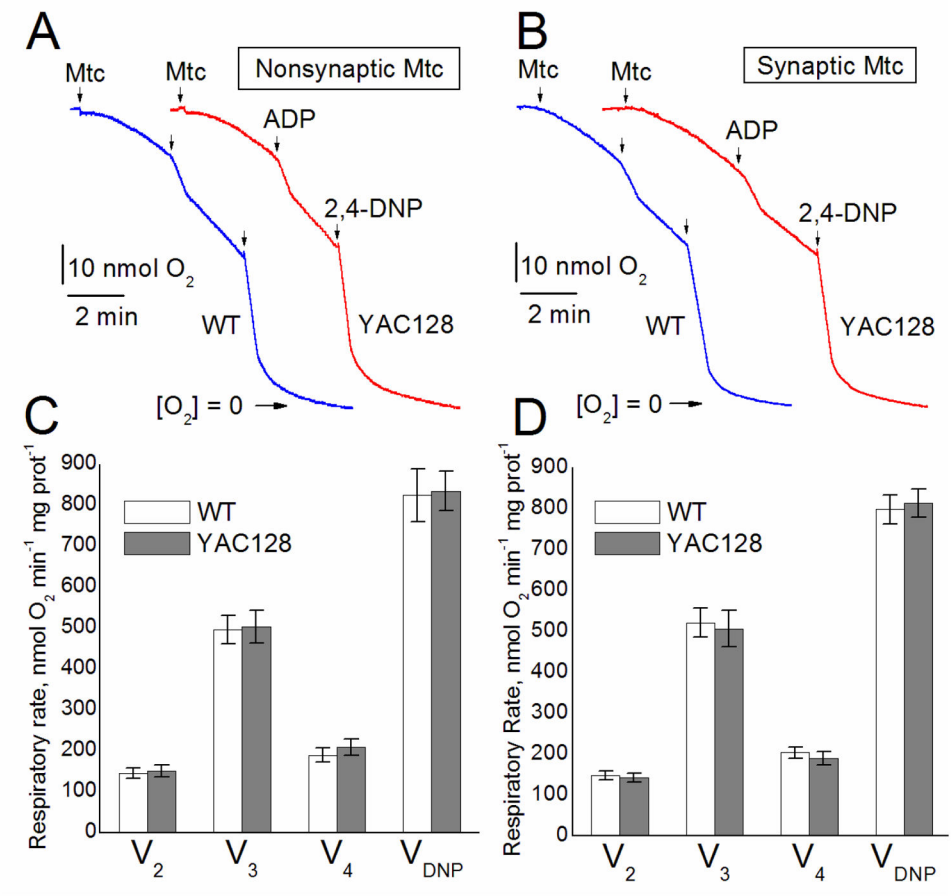

Figure 4.

Respiratory activity of striatal nonsynaptic and synaptic mitochondria isolated from 2-month-old FVB/NJ (blue traces) and YAC128 (red traces) mice. Representative traces of oxygen consumption by either striatal nonsynaptic (**A**) or striatal synaptic (**B**) mitochondria. Where indicated, mitochondria (30μg protein), 200μM ADP, or 60μM 2,4-dinitrophenol (2,4-DNP) were added. The incubation medium was supplemented with the Complex II substrate succinate (3mM) plus glutamate (3mM). Additionally, incubation medium was supplemented with 0.1% BSA (free from fatty acids) to maintain mitochondrial integrity (Lai and Clark, 1989). The pooled group results demonstrating respiratory rates are shown for striatal nonsynaptic (**C**) and striatal synaptic (**D**) mitochondria. Data are mean ± SEM, n = 5 (nonsynaptic), n = 4 (synaptic).

Author Manuscript Author Manuscript Author Manuscript Author Manuscript

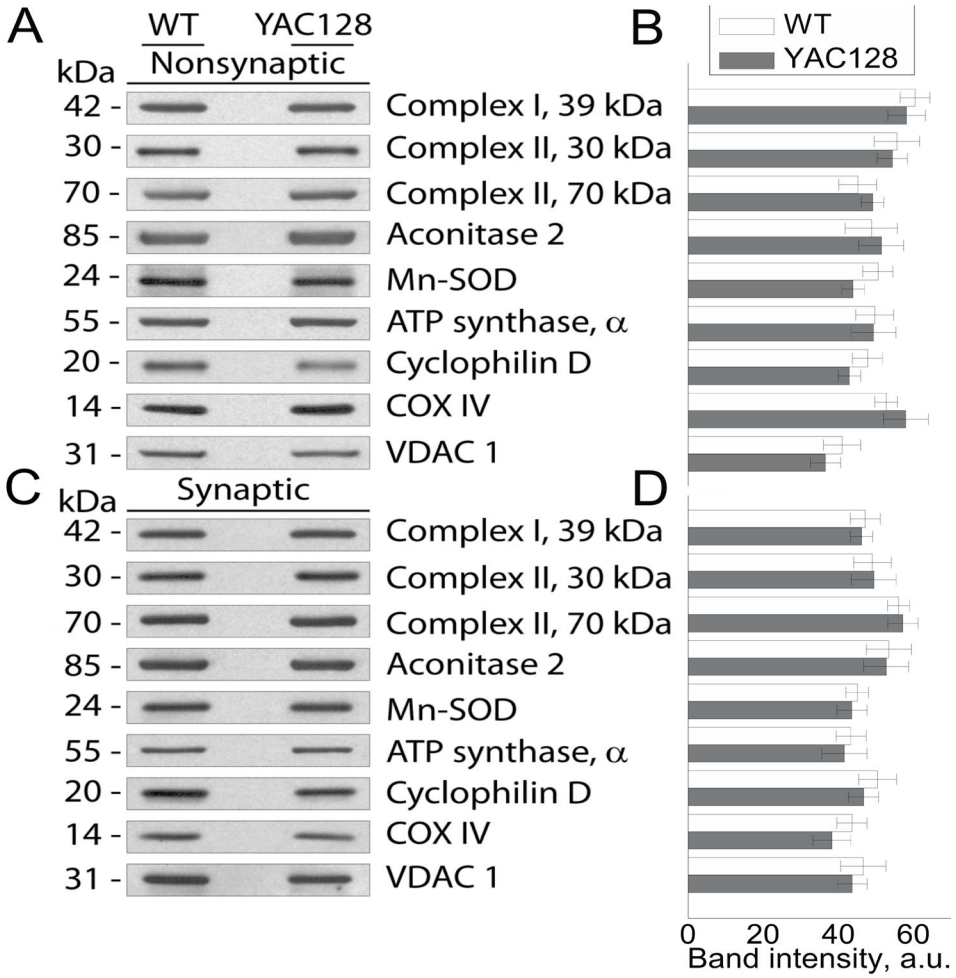

Figure 5.

Expression of nuclear encoded mitochondrial proteins in nonsynaptic and synaptic striatal mitochondria derived from FVB/NJ and YAC128 mice. In **A** and **C**, are representative western blots of nonsynaptic and synaptic striatal mitochondria isolated from FVB/NJ and YAC128 mice probed with various antibodies against nuclear-encoded mitochondrial proteins including 39 kDa subunit of Complex I, 30 and 70 kDa subunits of Complex II, Aconitase 2, Mn-dependent superoxide dismutase (Mn-SOD), α subunit of ATP synthase, cyclophilin D (CyD), and cytochrome oxidase subunit IV (COX IV). Voltage-dependent anion channel isoform 1 (VDAC1) was used as a loading control. In **B** and **D**, the results of densitometry performed with NIH ImageJ 1.48v software. Data are mean ± SEM, n = 6.

Author Manuscript Author Manuscript Author Manuscript Author Manuscript

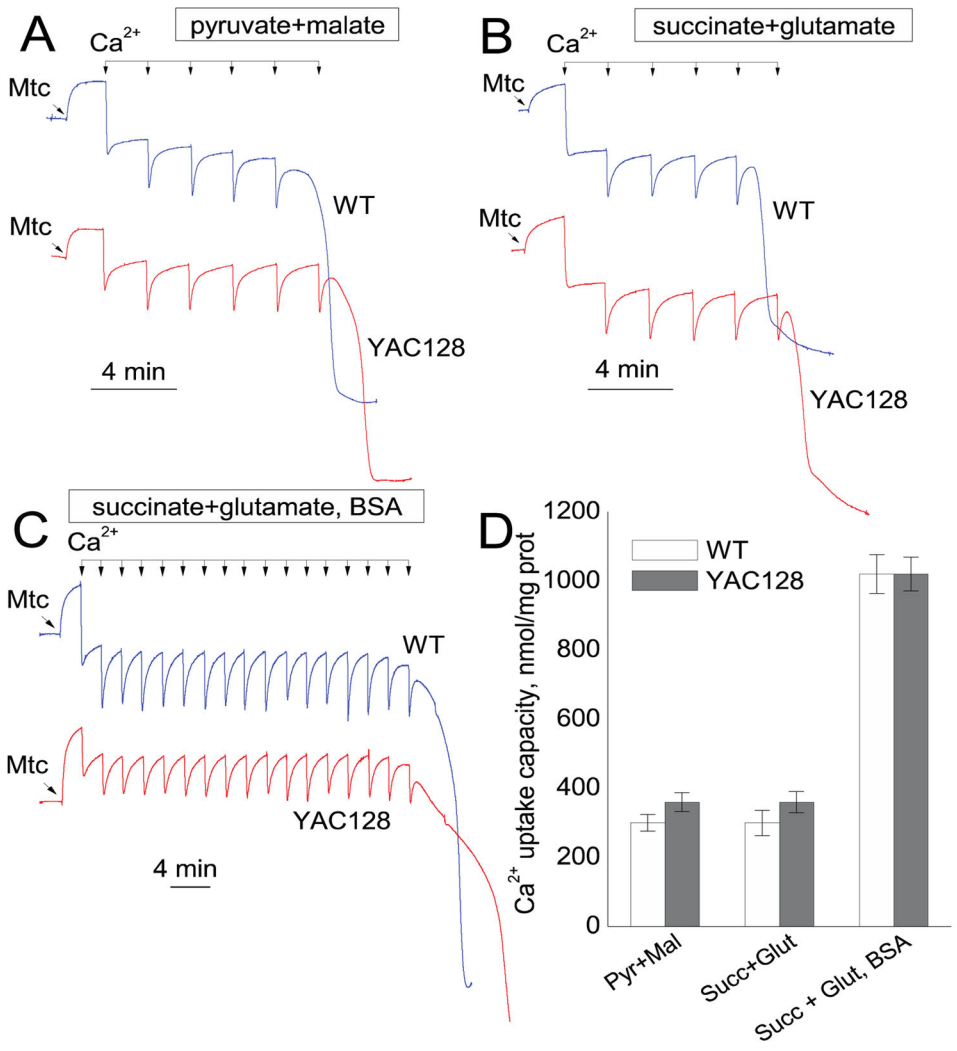

Figure 6.

Ca^{2+} uptake capacity of brain *nonsynaptic* mitochondria isolated from the striatum of FVB/NJ (blue traces) and YAC128 (red traces) mice. Mitochondrial Ca^{2+} uptake capacity was measured in the standard incubation medium supplemented with the Complex I substrates pyruvate (3 mM) and malate (1 mM) (**A**), or the Complex II substrate succinate plus glutamate (both in 3 mM) (**B**). In **C**, in addition to succinate plus glutamate, the incubation medium was supplemented with 0.1% BSA (free from fatty acids). In all experiments, the incubation medium was also supplemented with 100μM ADP and 1μM oligomycin (Chalmers and Nicholls, 2003). Where indicated, 10μM Ca^{2+} pulses (delivered as $CaCl_2$) were applied to mitochondria until mitochondria were unable to accumulate additional Ca^{2+} and released previously accumulated Ca^{2+}. In **D**, the pooled group results demonstrating Ca^{2+} uptake capacity of striatal nonsynaptic mitochondria from FVB/NJ and YAC128 mice. Data are mean ± SEM, n = 4.

Author Manuscript Author Manuscript Author Manuscript Author Manuscript

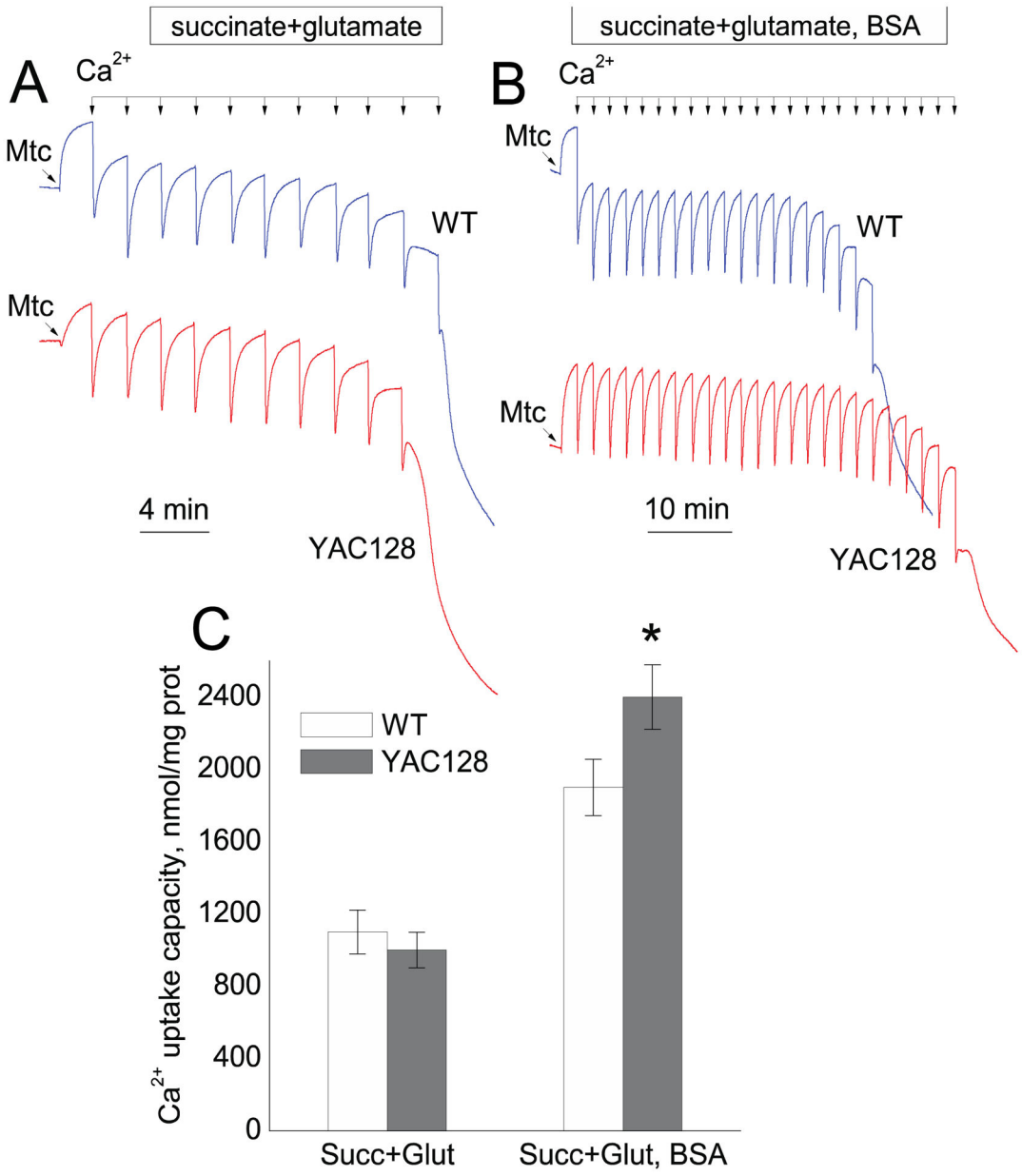

Figure 7.

Ca^{2+} uptake capacity of brain *synaptic* mitochondria isolated from the striatum of FVB/NJ (blue traces) and YAC128 (red traces) mice. Mitochondrial Ca^{2+} uptake capacity was measured in the standard incubation medium supplemented with the Complex II substrate succinate (3 mM) plus glutamate (3 mM) in the absence (**A**) or presence of 0.1% BSA (**B**). In all experiments, the incubation medium was also supplemented with 100μM ADP and 1μM oligomycin (Chalmers and Nicholls ,2003). Where indicated, 10μM Ca^{2+} pulses (delivered as $CaCl_2$) were applied to mitochondria until mitochondria were unable to accumulate additional Ca^{2+} and released previously accumulated Ca^{2+}. In **C**, the pooled group results showing Ca^{2+} uptake capacity of striatal synaptic mitochondria from FVB/NJ

and YAC128 mice. Data are mean ± SEM, *p<0.05 comparing mitochondria from YAC128 and FVB/NJ mice in the presence of 0.1% BSA, n = 5.

Author Manuscript Author Manuscript Author Manuscript Author Manuscript